

Figure S1. Related to Figure 1. Master transcription factor-driven transcription reprogramming and chromatin binding.

A, Percentage of MYOD-positive nuclei. (n=3). Data are represented as mean +/- standard error of the mean (SEM). Two-way ANOVA was used for statistical analysis, corrected for multiple testing (Tukey), *** p<0.001.

B, Percentage of nuclei in MyHC positive cells. (n=3). Data are represented as mean +/- standard error of the mean (SEM). Two-way ANOVA was used for statistical analysis, corrected for multiple testing (Tukey), *** p<0.001.

C, Immunoblot analysis of the whole cell lysate (left). Data is represented as mean +/- SEM.

D, Cell cycle analysis (n=3). Data is represented as mean +/- SEM.

E, Selected biological functions enriched by MYOD comparing MYOD GM vs EMPTY GM and MYOD DM vs EMPTY DM (IPA).

F, Percentage of up- or down-regulated genes in MYOD DM vs EMPTY GM that are common to up- or down-regulated genes in hMT vs EMPTY GM.

G, Relative expression of muscle, fibrotic and inflammatory genes (n=2-4) by RT-qPCR. Data is represented as mean +/- SEM. Two-way ANOVA was used for statistical analysis, corrected for multiple testing (Tukey), * p<0.05, ** p<0.01, *** p<0.001.

H, Upstream prediction analysis by IPA based on the gene expression profile of MEFs and MEF-derived iPSCs. All categories have p< 1x10⁻⁷.

I, E-box motif enrichment (left) and distribution (right) at +/-50bp from MYOD peak summit, in GM (top) and DM (bottom).

J, UCSC snapshot of MYOD ChIP-seq in MYOD GM and in MYOD DM on *SMARCD3* (top) or *MYOG* (bottom) loci.

K, Percentage of up- (black) or down- (grey) regulated genes during commitment and differentiation (All DE genes). Percentage of MYOD-bound up- or down-regulated genes during commitment and differentiation (MYOD-bound DE genes).

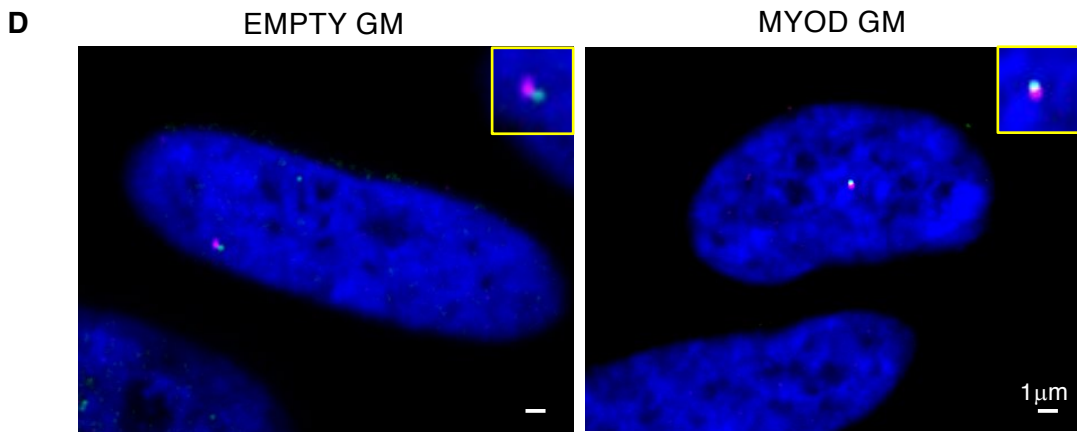
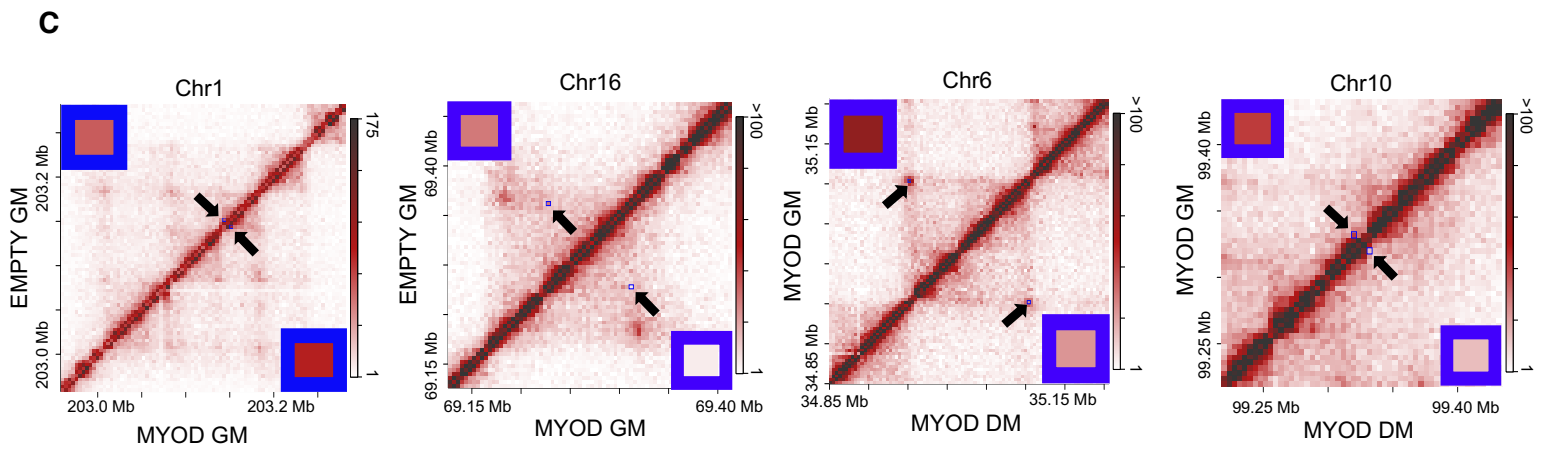
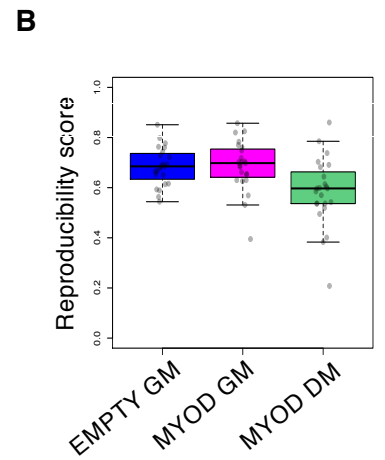
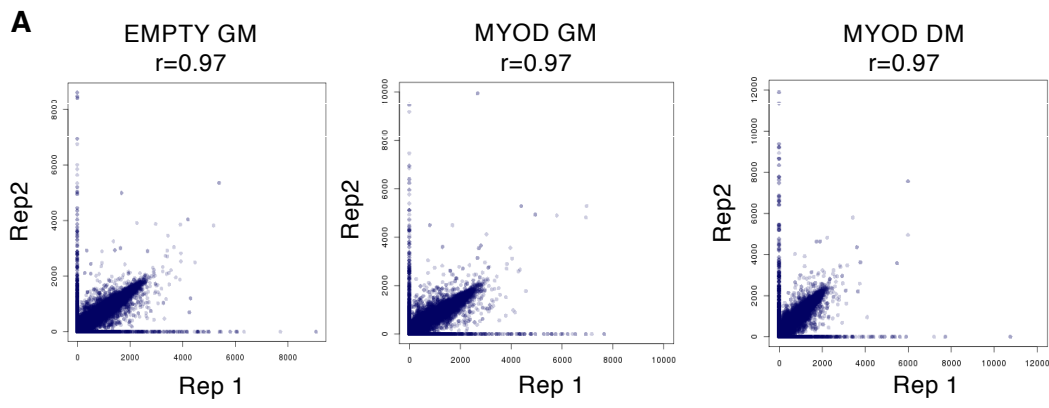


Figure S2. Related to Figure 2. Hi-C Reproducibility and examples of differential interactions.

A, Scatter plot representing reproducibility of two biological replicates as in Dixon et al, 2012.

B. Reproducibility score of intra-chromosomal Hi-C contact matrices among biological replicates calculated using HiC-spector. Each chromosome is represented as a single circle.

C, Normalized Hi-C contact heatmaps for EMPTY GM (top left) vs MYOD GM (bottom right), and for MYOD GM (top left) vs MYOD DM (bottom right). Interaction under investigation is highlighted by blue boxes. Magnification of the blue boxes is shown on the corners of each heatmap.

D, Left: illustrative images of DNA FISH for two probes (green and red) spanning 100kb regions centered around two 4kb regions that differentially interacted with each other between EMPTY GM and MYOD GM. DNA is stained with Hoechst. Right: distance between DNA FISH probes.

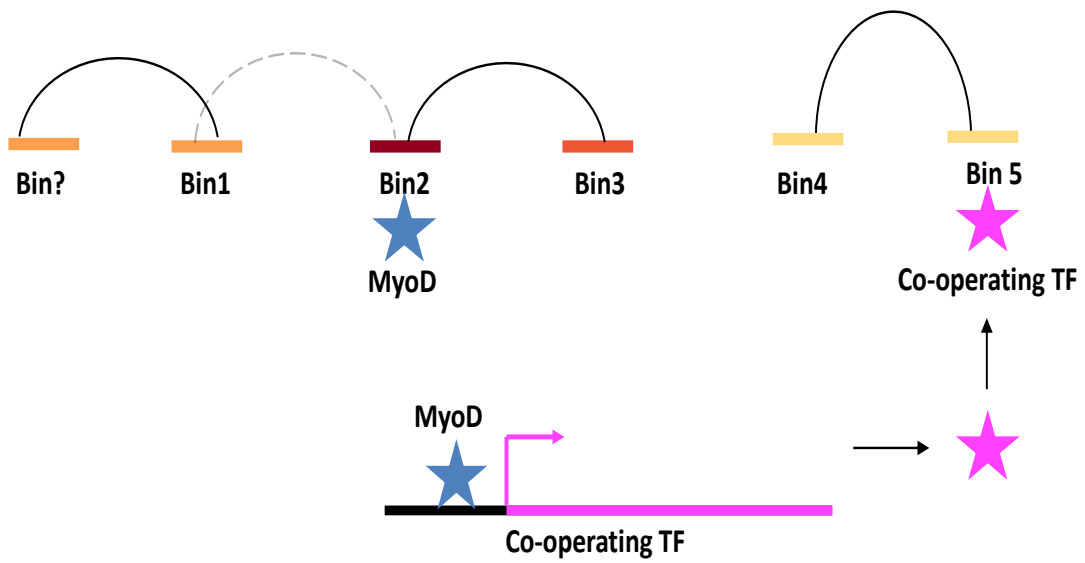
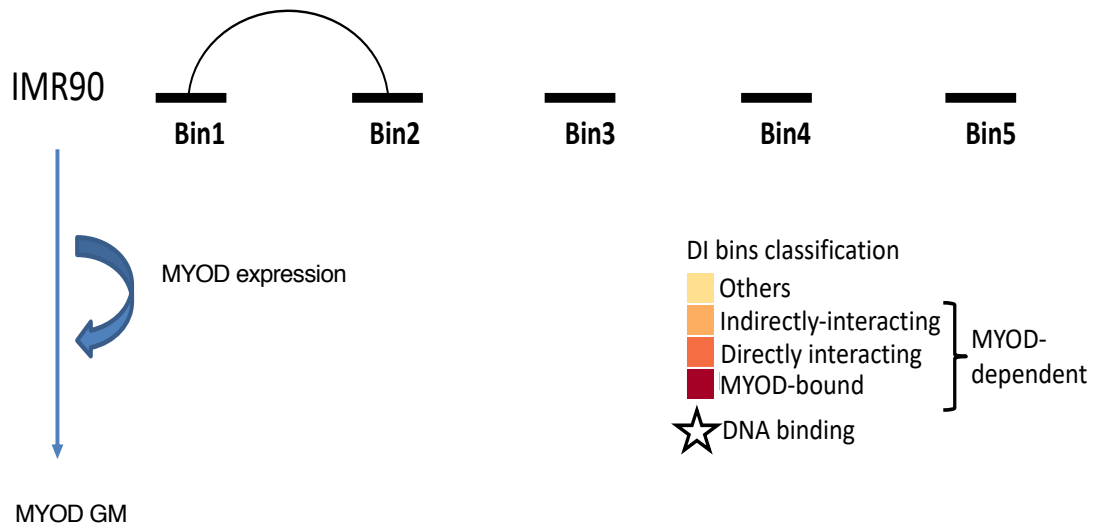
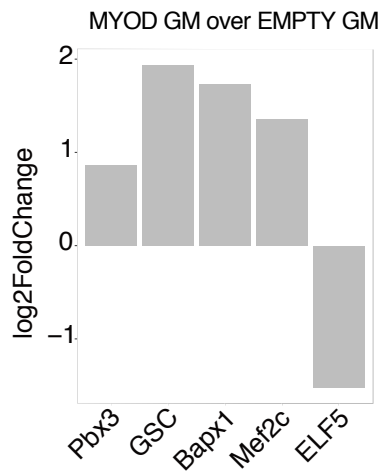
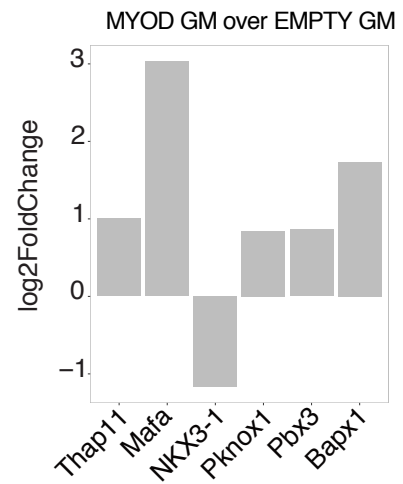
A**B****C**

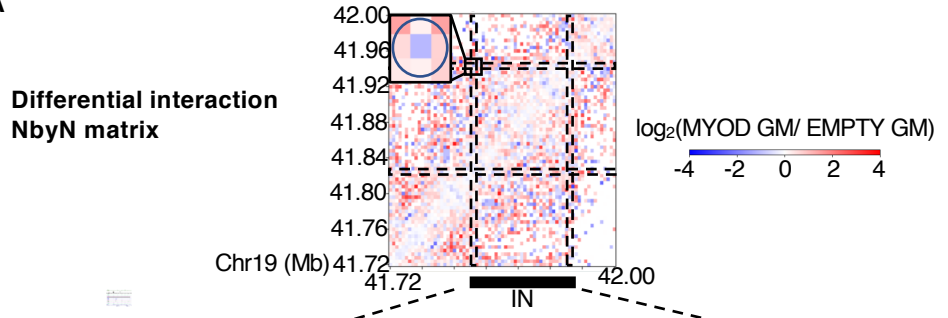
Figure S3. Related to Figure 2. MYOD-domino effect of differential interactions.

A, Schematic representation of MYOD-domino effect on differential chromatin interactions.

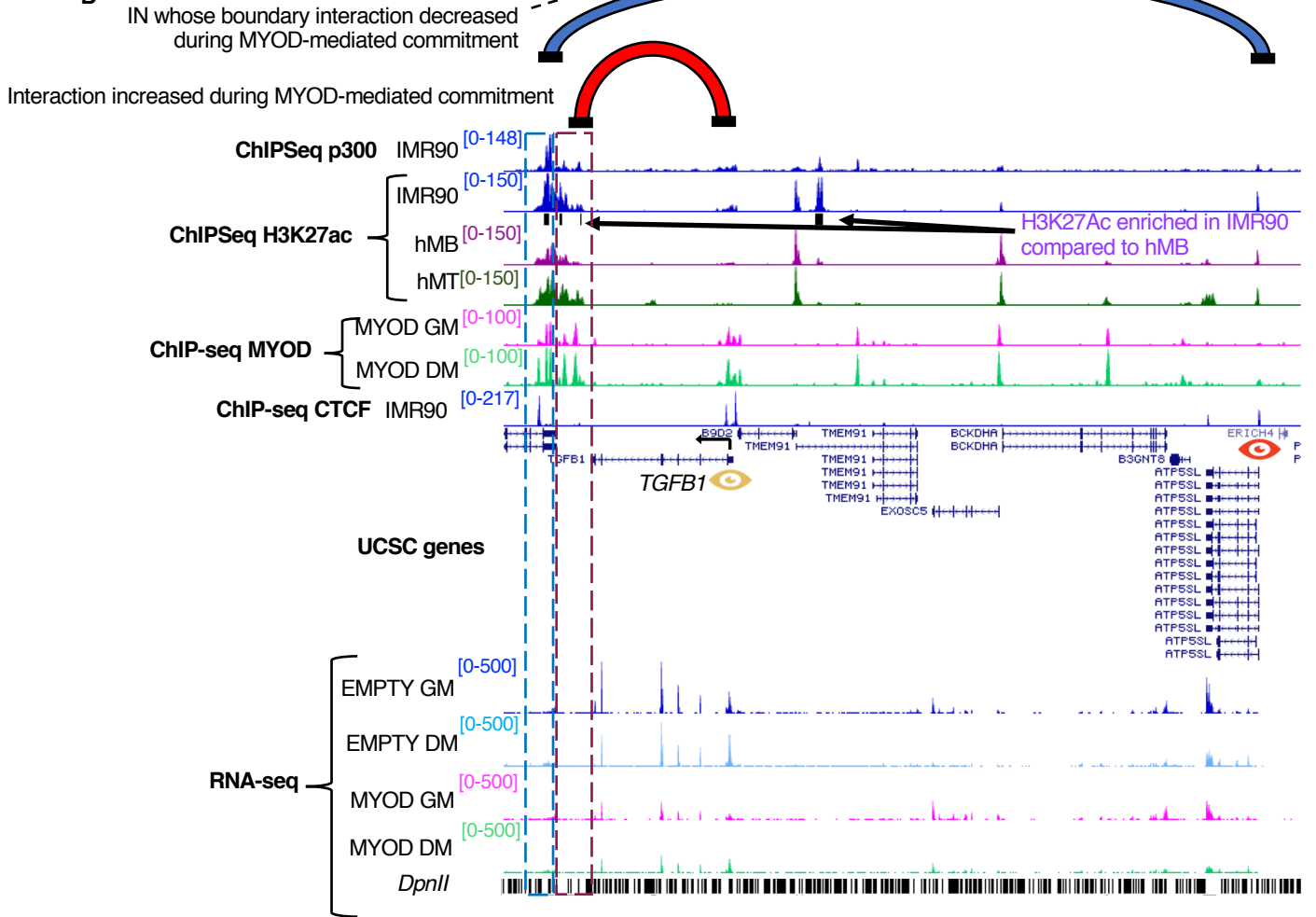
B, Differential gene expression by RNA-seq of TFs whose DNA binding motif is present around the TSS located inside directly interacting bins (left). The directly interacting bins refer to Fig 2F EMPTY GM vs MYOD GM.

C, Differential gene expression by RNA-seq of TFs whose DNA binding motif is present around the TSS contained within indirectly-interacting bins and other bins (right). indirectly-interacting bins and other bins refer to Fig 2F EMPTY GM vs MYOD GM.

A



B



C

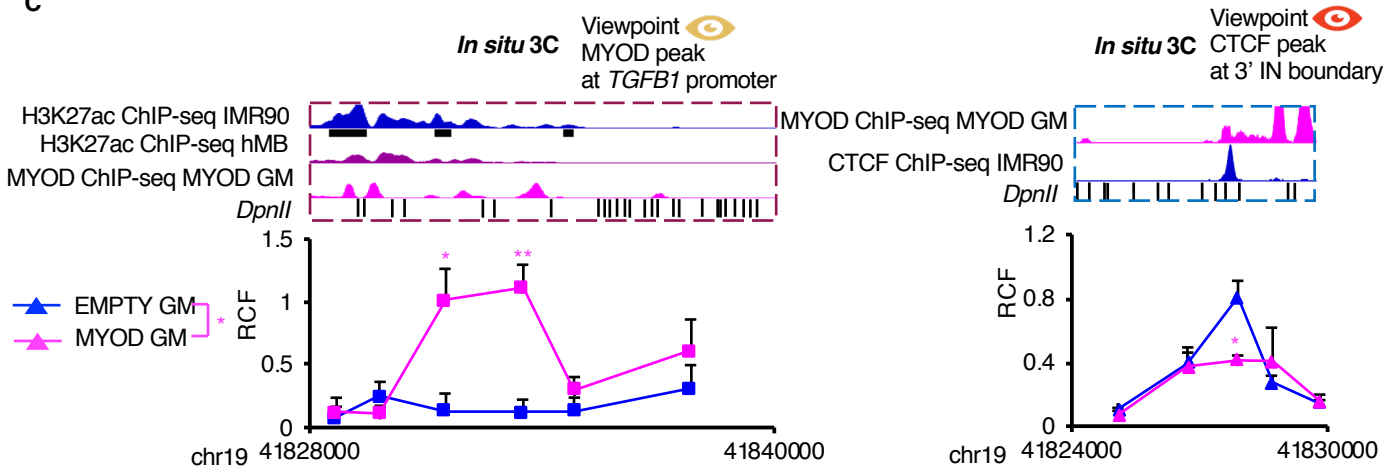


Figure S4. Related to Figure 4. 3D Regulation of *TGF-β1* Expression.

A, Differential interaction NbyN map of *TGF-β1* locus and location of altered IN during MYOD-mediated commitment (black bar).

B, From top to bottom: blue arch representing decreased interaction between two IN boundaries (CTCF-bound bins) during MYOD-mediated commitment, red arch representing an increased interaction during MYOD-mediated commitment, UCSC snapshot of p300 ChIP-seq in IMR90 (blue), H3K27ac ChIP-seq in IMR90 (blue), H3K27ac ChIP-seq peaks enriched in IMR90 as compared to hMB and hMT (black bars), H3K27Ac ChIP-Seq in hMB, H3K27Ac ChIP-Seq in hMT, MYOD ChIP-seq in MYOD GM (magenta) and MYOD DM (light green), CTCF ChIP-seq in IMR90 (blue), RefSeq genes from UCSC browser, RNASeq of EMPTY GM (blue), EMPTY DM (light blue), MYOD GM (magenta), MYOD DM (light green). DpnII digestion sites (black)

C, Left: Close up representation of the DNA regions delimited by violet dashed box in (B), from top to bottom: H3K27ac ChIP-seq in IMR90 (blue) and hMB (violet), MYOD ChIP-seq in MYOD GM (magenta), DpnII sites, relative crosslinking frequencies (RCF) by in situ 3C using as view point MYOD peak at *TGF-β1* promoter (gold eye) and measuring RCF with DpnII fragments above. Right: Close up representation of the DNA regions delimited by blue dashed box in (B), from top to bottom: MYOD ChIP-seq in MYOD GM (magenta), CTCF ChIP-seq in IMR90 (blue) and DpnII sites. Relative crosslinking frequencies (RCF) by in situ 3C using as view point CTCF peak at IN boundaries containing *TGF-β1* (red eye) and measuring RCF with DpnII fragments above (n=3). 3C data is represented as mean + SEM. T-test was used for statistical analysis, * p<0.05, ** p<0.01.

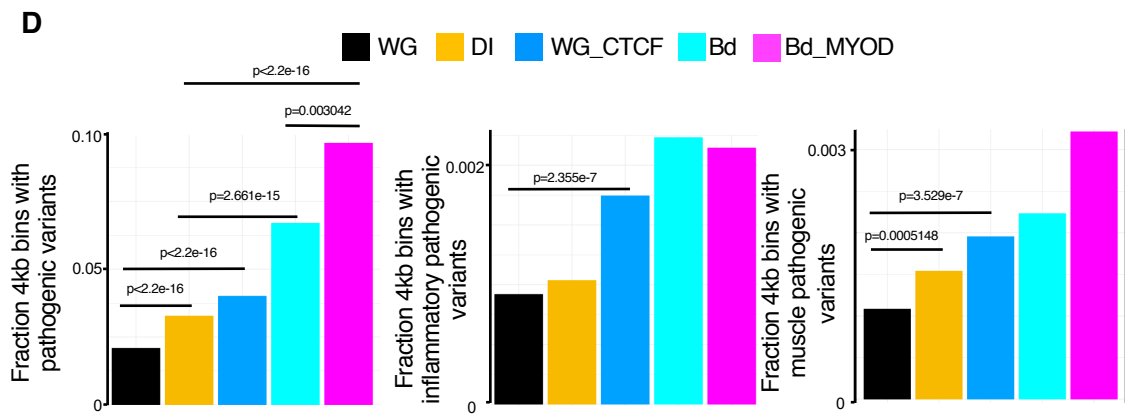
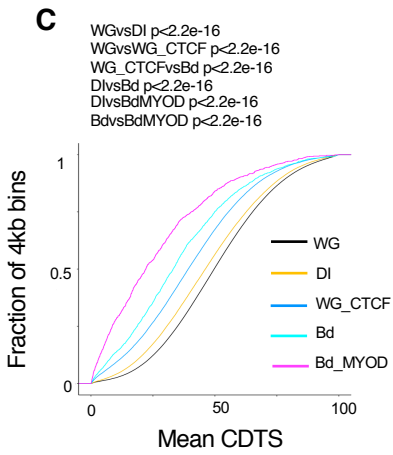
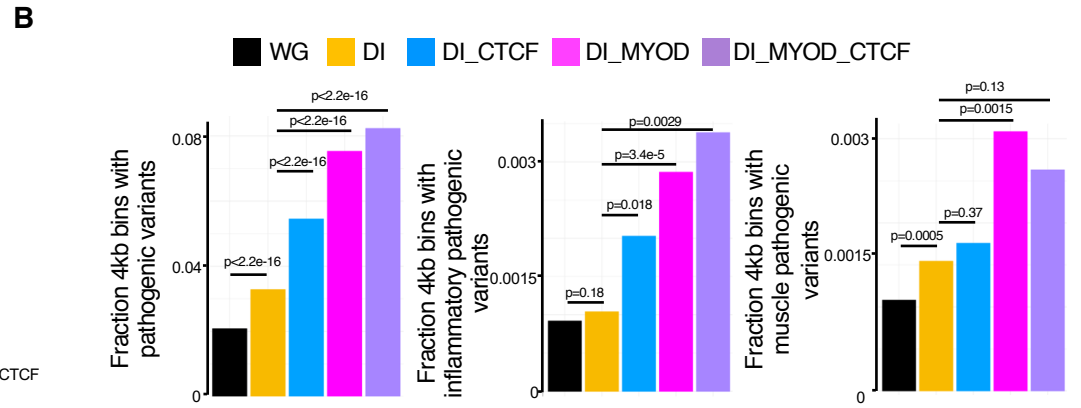
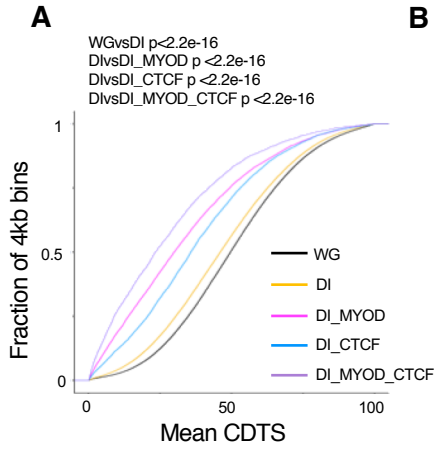


Figure S5. Related to Figure 2 and 4. MYOD-bound differentially interacting elements are highly constraint and enriched in annotated pathogenic variants.

A, DNA sequence constraint of all bins genome-wide bins (WG, black), differentially interacting bins (DI, yellow), MYOD-bound bins DI bins (DI_MYOD, magenta), CTCF-bound DI bins (DI_CTCF, light blue) or MYOD and CTCF bound DI bins (DI_MYOD_CTCF, purple). Two-sample Kolmogorov-Smirnov test was used for statistical analysis.

B, Fraction of genome-wide bins (WG, black), differentially interacting bins (DI, yellow), MYOD-bound bins DI bins (DI_MYOD, magenta), CTCF-bound DI bins (DI_CTCF, light blue) or MYOD and CTCF bound DI bins (DI_MYOD_CTCF, purple) harboring variants associated to all diseases (left), inflammatory diseases (middle) or muscle diseases (right). One sided Fisher's Exact Test was used for all statistical analysis in the figure.

C, DNA sequence constraint of all bins genome-wide (WG), differentially interacting bins (DI), CTCF-bound bins (WG_CTCF), differentially interacting bins co-bound by CTCF (Bd), and differentially interacting bins co-bound by CTCF and bound by MYOD (Bd_MYOD). Two-sample Kolmogorov-Smirnov test was used for statistical analysis.

D, Fraction of genome-wide (WG), differentially interacting bins (DI), CTCF-bound bins (WG_CTCF), differentially interacting bins co-bound by CTCF (Bd), and differentially interacting bins co-bound by CTCF and bound by MYOD (Bd_MYOD) harboring annotated pathogenic variants associated to all annotated diseases (left), inflammatory (middle) or muscle diseases (right). One sided Fisher's Exact Test was used for all statistical analysis in the figure.

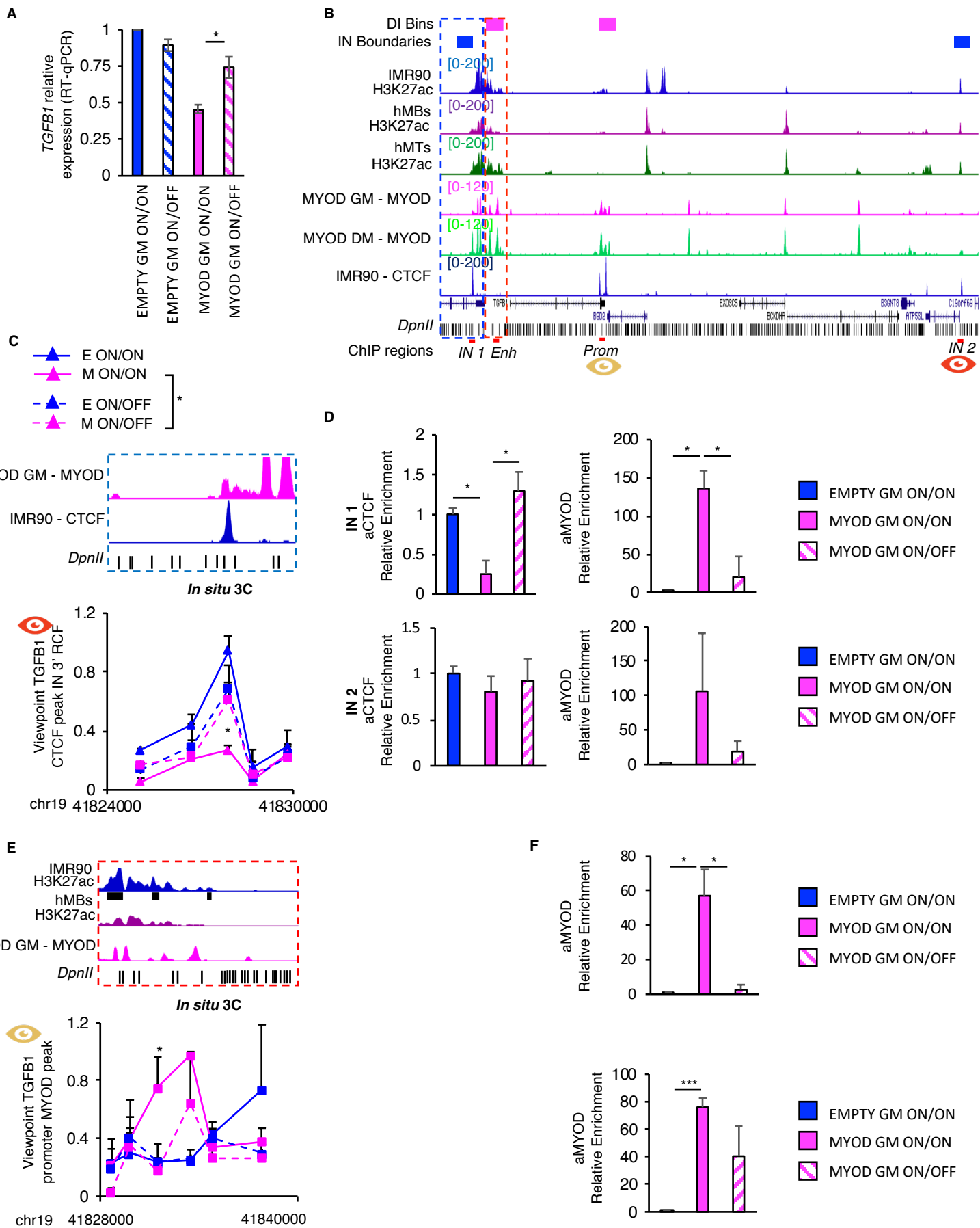


Figure S6. Related to Figure 5. Requirement of *Myod1* expression for maintaining myogenic 3D interaction.

A, Relative mRNA expression of *TGF- β 1* compared to EMPTY ON/ON (n=3). Data is represented as mean +/- SEM.

B, From top to bottom: magenta boxes representing bins with an increased interaction during MYOD-mediated commitment; blue boxes representing bins with decreased interaction between two IN boundaries (CTCF-bound bins) during MYOD-mediated commitment; UCSC snapshot of H3K27ac ChIP-seq in IMR90 (blue), in hMBs (purple) and in hMTs (dark green); MYOD ChIP-seq in MYOD GM (magenta) and MYOD DM (light green); CTCF ChIP-seq in IMR90 (blue); RefSeq genes; DpnII digestion sites (black); regions analyzed by ChIP-qPCR; eyes are viewpoints for 3C experiments.

C, From top to bottom: UCSC snapshot of the same region that in panel (B) within dashed blue box, MYOD ChIP-seq in MYOD GM; CTCF ChIP-seq in IMR90; DpnII sites; RCF values between CTCF peak at 5' the region of an altered IN containing *TGF- β 1* (view point – red eye – see panel B) and the CTCF peak at 3' region after 1 day of doxycycline treatment and 2 days with/out doxycycline treatment (ON/ON, ON/OFF). Data is represented as mean + SEM (n=3).

D, ChIP-qPCR analysis for CTCF, MYOD enrichment on the IN1 region (top panels) and on the IN2 region (bottom panels). Data are shown as relative enrichment to EMPTY ON/OFF, as mean +/- SEM (n=2).

E, From top to bottom: UCSC snapshot of the same region that in panel (B) within dashed red box, H3K27ac ChIP-seq in IMR90; H3K27ac ChIP-seq in hMBs; MYOD ChIP-seq in MYOD GM; DpnII sites; RCF values between a DpnII fragment containing MYOD peak in the promoter of *TGF- β 1* (view point – gold eye – see panel B) and an enhancer located at the 3' of the gene after 1 day of doxycycline treatment and 2 days with/out doxycycline treatment (ON/ON, ON/OFF). (Right panel) Data is represented as mean + SEM (n=3).

F, ChIP-qPCR analysis for MYOD enrichment on the *TGF- β 1* promoter region (top panel) and on the Enhancer region (bottom panel). Data are shown as relative enrichment to EMPTY ON/OFF, as mean +/- SEM (n=2).

T-test was used for statistical analysis, * p<0.05, ** p<0.01.

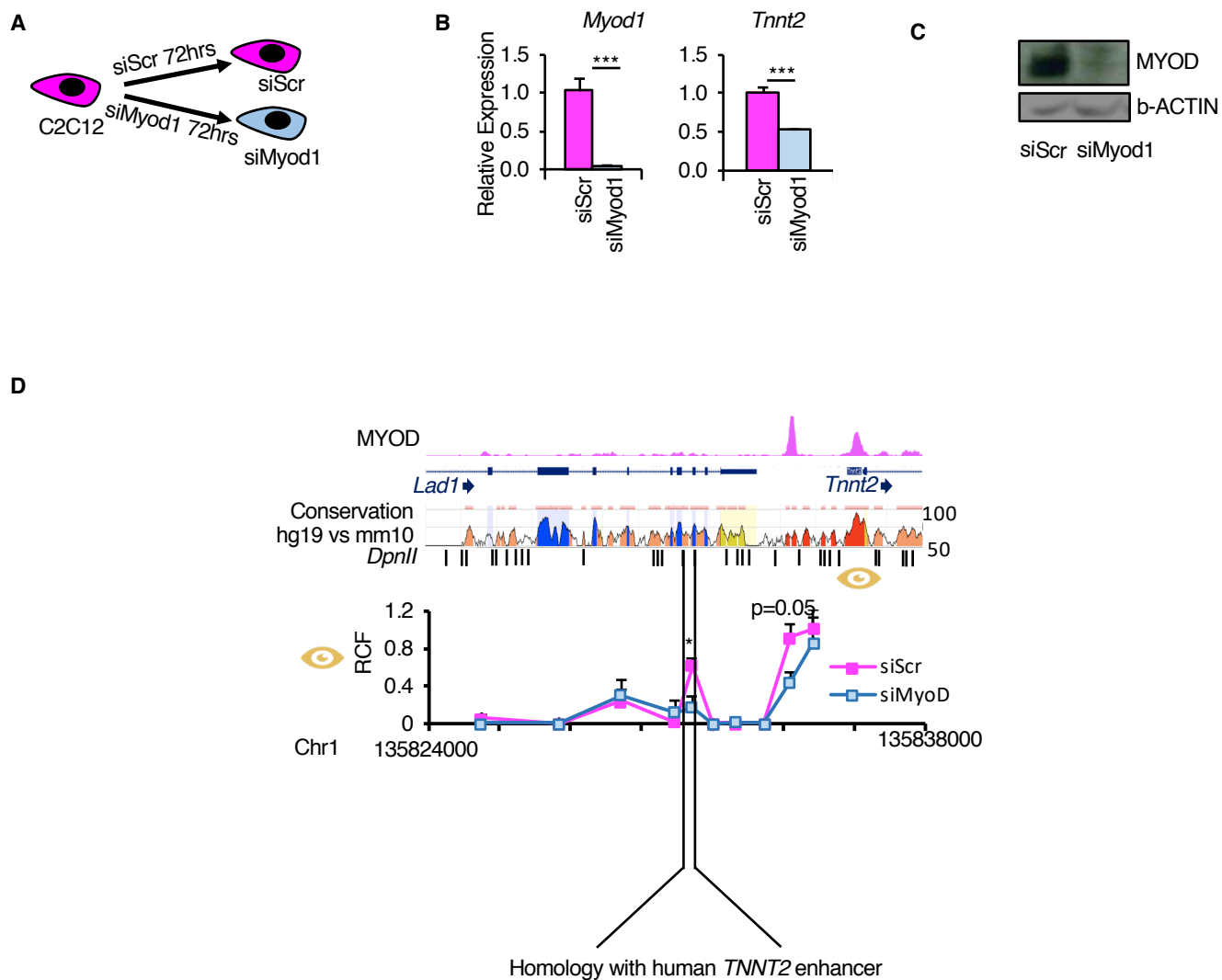


Figure S7. Related to Fig. 5. MYOD mechanisms to regulate gene expression conserved between human and mouse.

A, Scheme of the experimental approach in C2C12. C2C12 cells were kept non-confluent and transfected with siRNA scramble (siScr) or siRNA targeting *Myod1* (siMyod1) for 72h.

B, Relative mRNA expression of *Myod1*, *Tnnt2* (n=3). Data is represented as mean +/- SEM. *** p<0.001

C, Immunoblot analysis of the whole cell lysate. b-ACTIN is used as loading control.

D, From top to bottom: UCSC snapshot of MYOD ChIP-seq in C2C12 myoblasts, UCSC genes (arrow indicates transcription direction), conservation levels between human and mouse genomes, DpnII sites, RCF values between MYOD peak at *Tnnt2* promoter (view point - gold eye symbol) and mouse homolog region to the human *TNNT2* enhancer. Data is represented as mean + SEM (n=3).

Motif	TF	p-value
	CTCF	1e-52
	Boris/CTCF	1e-23
	Myf5	1e-9
	MyoG	1e-8
	MyoD	1e-8
	Atoh1	1e-7
	Tcf12	1e-7
	Fli1	1e-7
	NeuroD1	1e-6
	Ap4	1e-5
	Fra2	1e-5
	Tcf21	1e-4
	TEAD2	1e-4
	Jun-AP1	1e-4
	Olig2	1e-4
	Fosl2	1e-4
	Fra1	1e-4
	Ascl1	1e-4
	Bach2	1e-4
	NeuroG2	1e-3

Table S2. Related to Fig. 4. Motif analysis at increased IN boundary interactions.

HOMER motif analysis at the center of MYOD peaks (+/-500bp) that mapped at IN boundaries with strengthened interaction bound by MYOD at both sides during MYOD-mediated commitment

Motif	TF	p-value
	CTCF	1e-37
	Boris/CTCFL	1e-23
	Ap4	1e-4
	KLF6	1e-4
	Elk1	1e-4
	MyoG	1e-3
	Ets1-distal	1e-3
	MyoD	1e-3
	Egr1	1e-3
	KLF14	1e-2
	E2F3	1e-2
	NeuroD1	1e-2
	Sp5	1e-2
	EWS:FLI1-fusion	1e-2
	GABPA	1e-2
	Tcf12	1e-2
	Tcf21	1e-2
	Foxo1	1e-2
	Foxa3	1e-2
	Myf5	1e-2

Table S3. Related to Fig. 4. Motif analysis at decreased IN boundary interactions.

HOMER motif analysis at the center of MYOD peaks (+/-500bp) that mapped at IN boundaries with weakened interaction bound by MYOD at both sides during MYOD-mediated commitment

Primer Name	Primer Sequence
mouse MYOD mRNA For	AGCACTACAGTGGCGACTCA
mouse MYOD mRNA Rev	GGCCGCTGTAATCCATCAT
hGAPDH mRNA For	GAAGGTGAAGGTCGGAGTC
hGAPDH mRNA Rev	GAAGATGGTGATGGGATTTTC
hGAPDH premRNA Rev	CCATACGACTGCAAAGACCC
hbeta-actin mRNA For	CCTGGGCATGGAGTCCTGTGG
hbeta-actin mRNA Rev	CTGTGTTGGCGTACAGGTCTT
hMYOG mRNA For	AATGCAGCTCTCACAGCGCCTC
hMYOG mRNA Rev	TCAGCCGTGAGCAGATGATCC
hMYHC1 mRNA For	CGAAGCTGGAGCTACTGTAA
hMYHC1 mRNA Rev	CCATGTCTCGATCTTGTGATA
hCKM mRNA For	TGGAGAAGCTCTCTGTGGAAG
hCKM mRNA Rev	TCCGTCATGCTCTCAGAGGGT
hTGF- β 1 mRNA For	GCCTGAGGCCGACTACTA
hTGF- β 1 mRNA Rev	CTGTGTGTA CTCTGCTTGA ACT
hCTGF mRNA For	TGTGCACCGCCAAAGAT
hCTGF mRNA Rev	GCACGTGCACTGGTACTT
hPOSTN mRNA For	CTGCTTATTGTTAACCCATATAAACGC
hPOSTN mRNA Rev	CAGACATTTGGGCCTTGGT
hIL6 mRNA For	CGGGAACGAAAGAGAAGCTCTA
hIL6 mRNA Rev	GGCGCTTGTGGAGAAGGAG
hVCAM1 mRNA For	CCGATTGCTGCTCAGATTG
hVCAM1 mRNA Rev	AGCGTGGAATTGGTCCCCTCA
hIL1b mRNA For	CATCTACGAATCTCCGACCAC
hIL1b mRNA Rev	GGCAGGGAACCAGCATCTTC
hTNNT2 mRNA For	TCAAAGTCCACTCTCTCCATC
hTNNT2 mRNA Rev	GGAGGAGTCCAAACCAAAGCC
hCTCF mRNA For	GTGGCGCGGAGAATGATTA
hCTCF mRNA Rev	AATAGAACCCAGCTCTCAAGC
hITGA7 mRNA For	CGCCTTCAATCTGGACGTGA
hITGA7 mRNA Rev	CCCACCAGCAGCCAGC
hRDH5 mRNA For	TTAGTGTGGGAGGCTGGGAA
hRDH5 mRNA Rev	GTGGCAGCCTCCTGTGG
hBLOC1S1 mRNA For	CAGGCACTCAAGGAAATTGGG
hBLOC1S1 mRNA Rev	GACTGCAGCTGCCCTTTGTA
hLAD1 mRNA For	CACGGCCATACGGAGATCAG
hLAD1 mRNA Rev	TTCTCAAAGAGGTGGCGCTT
hTNNI1 mRNA For	GAGGTGTTCCAACCTGGGAG
hTNNI1 mRNA Rev	ACGCATACACACCATGCTCA
hPKP1 mRNA For	ACCGCGTCATCATTCCCTTC
hPKP1 mRNA Rev	AGCTCAGGTTCTCAAGCAG
hIGFN1 mRNA For	CAGCTGTACACCCAGGGTAAT
hIGFN1 mRNA Rev	TCACTCCAGGGATGTGGGAC
hSARNP mRNA For	TCTTGCTCGTGGTTTGAGA
hSARNP mRNA Rev	TTTGCCTCCTCTTCAGCATGT
mouse b-actin mRNA For	GGCTGTATTCCCCTCCATCG
mouse b-actin mRNA Rev	CCAGTTGGTAACAATGCCATGT
mouse Tnnt2 mRNA For	CAGAGGAGGCCAACGTAGAAG
mouse Tnnt2 mRNA Rev	CTCCATCGGGGATCTTGGGT

Table S4. Related to STAR Methods. Primers for gene expression.

Name and sequence of primers used for RT-qPCR experiments.

Primer Name	Primer Sequence
hTNNT2 promoter For	GCAGAGGGCAAGAGTTATGT
hTNNT2 promoter Rev	AAGGCTGCTCAGTCCATTAG
hTNNT2 enhancer For	TCACATGCTGTTCCCTCTATTT
hTNNT2 enhancer Rev	GGTGTCATGGAGCAATTGATTT
hIL6 promoter For	CTTCGGTCCAGTTGCCTTC
hIL6 promoter Rev	GCGGCTACATCTTTGGAATCT
hTGF- β 1 promoter For	GTCACCAGAGAAAGAGGACCAG
hTGF- β 1 promoter Rev	CTACCTTGTTTTCCAGCCTGA
hTGF- β 1 enhancer For	CAAAACAGACCCACACA ACTCC
hTGF- β 1 enhancer Rev	CAGTGTTTGTCTGTGTGAGGG
hTGF- β 1 IN5 For	CGTCAA AATGTCAA AATGCCGT
hTGF- β 1 IN5 Rev	TTACATTCTCAAGCAGGCAGTG
hTGF- β 1 IN3 For	TGAGCTTCAA AACGAGACACAG
hTGF- β 1 IN3 Rev	GGTTGCCCTATTTCTTTGTGGA
hITGA7 promoter For	ACCCATCACGTCCAGATTGAAG
hITGA7 promoter Rev	CTCCGGGATTTGCTACCTTTT
hITGA7 enhancer For	CTGTAGGTC ACTTGGGCTCC
hITGA7 enhancer For	CGGTGATGAAGACAAAGGCATT

Table S5. Related to STAR Methods. Primers for ChIP-qPCR.
Name and sequence of primers used for ChIP-qPCR experiments.

Primer Name	Primer Sequence	Genomic Coordinates
		DpnII Fragment
Human hg19		
3C_LoadingCtrl_F	AATGGGCTTAATGGAAGACAAAT	chr12 6632801 6634701
3C_LoadingCtrl_R	TGTGCTTAAATTCGGTCATCT	chr12 6632801 6634701
TNNT2_201347539 Viewpoint MYOD peak	GTCATCCCCTAACGGCTTAAAA	chr1 201346773 201347562
TNNT2_201346763 Viewpoint CTCF peak	GAGCCTTACCTCAGAACAGCAG	chr1 201345693 201346776
TNNT2_201354973	AGTGTACATAAGAGGTCTAGGG	chr1 201354133 201355158
TNNT2_201356497	AAGGTATCATCTGAGCAAAGCAC	chr1 201355155 201356621
TNNT2_201352732	TTCCAAGAAACGTCCCATCAAT	chr1 201352335 201352895
TNNT2_201351662	CTCCTGAAATGACTCCTCCTCTC	chr1 201350893 201351795
TNNT2_201349564	AACTCTCGGCTATGAAGTTGGAA	chr1 201348865 201349739
TNNT2_201357190	CCCCACCTCATAATCCCAAATC	chr1 201356659 201357298
TNNT2_201354065	AAGACATGTCTCCTCCTCTTC	chr1 201353778 201354136
TNNT2_201353395	AGTAAATGTTTCATGGGGCAGATG	chr1 201352950 201353451
TNNT2_201353646	CCTTTCCTGTCTAACCTCAAG	chr1 201353448 201353713
TNNT2_201352338	ACAGGAGCCACGAATAACTCAG	chr1 201351817 201352338
TGF-β1_41946123 Viewpoint IN	TCTCCACAAAGAAATAGGGCAAC	chr19 41946101 41946123
TGF-β1_41827968	TTGAGAAATGAAGCCCATGTGTC	chr19 41827946 41827968
TGF-β1_41827078	CATCAGGAAAGTGGGAATTGTGA	chr19 41827056 41827078
TGF-β1_41825348	CCTGCATGTTTTCTGTGTTTT	chr19 41825327 41825348
TGF-β1_41829197	TTAGTTCCCATCTCTCCTCTCTG	chr19 41829175 41829197
TGF-β1_41830037	CAACCAGAATTAGAGCCAGACAG	chr19 41830015 41830037
TGF-β1_41859165 Viewpoint Prom	TCCCACGGAAATAACCTAGATG	chr19 41858791 41859165
TGF-β1_41832499	CTGAGAACCACAGGAAGCATG	chr19 41830487 41832499
TGF-β1_41834210	GATGTACAGACTGAGTGGGTAAGA	chr19 41832786 41834210
TGF-β1_41835463	CACCACAATGCCAGACTAATTTT	chr19 41834207 41835463
TGF-β1_41838117	CCAACTCACCTCTCTGACTTTAC	chr19 41837557 41838117
ITGA7_56100255 Viewpoint	ACAGTAGAGGCAGAAGACAGTC	chr12 56099397 56100255
ITGA7_56112320	TAACCACAGCCCATACCTTGAT	chr12 56111586 56112320
ITGA7_56114416	GGAAGTGAAGACTAGCCAGA	chr12 56112971 56114416
ITGA7_56115224	CAGAGAGGCTTCCGAGTCC	chr12 56114729 56115224
ITGA7_56115639	CGGGTGCTGAATGTGAACAC	chr12 56115321 56115639
Mouse mm10		
3C_loadingCtrl_mm_F	GAACGGTACCACACTCAGTTTAC	chr5 142911269 142911402
3C_loadingCtrl_mm_R	AGACCTGACTCTTCAAGCTATCA	chr5 142911269 142911402
Tnnt2_135836700 Viewpoint Myod	TGTTTCCAGGACAGACTCTAACA	chr1 135835646 135836700
Tnnt2_135835151	CACACATGTCTCAGGATAAGCC	chr1 135834524 135835151
Tnnt2_135834527 Viewpoint CTCF	GTGTAGGAGGTGACATTTGAGTG	chr1 135833823 135834527
Tnnt2_135833826	CCCTTTGTCTTAGGCCCTATAGT	chr1 135833115 135833826
Tnnt2_135832869	AGTGCTAGACCTATTTACCGCTC	chr1 135832431 135832869
Tnnt2_135832434	TCCCTTTCCTTGTCTAATTGGC	chr1 135831572 135832434
Tnnt2_135831575	CGTGACATCAAGACTTAACTGT	chr1 135831231 135831575
Tnnt2_135831234	GTAAGTGAAGTCTTGTACACCT	chr1 135830616 135831234
Tnnt2_135830422	GCAAGAGGAGAACAATGACAAGA	chr1 135828430 135830422
Tnnt2_135828433	GGTAGCCTAGACTCCTGTTTTCT	chr1 135826900 135828433
Tnnt2_135825883	CCTGAGTTCAACCACAGATGATG	chr1 135825088 135825883

Table S6. Related to STAR Methods. Primers for 3C.

Name and sequence of primers used for 3C experiments and genomic coordinate of the DpnII fragment of interest.

Name	Sequence	PAM	Coordinates
TNNT2_M1	CAGCAGCTGCCGACAGATCC	TGG	chr1 201346758 201346777
TNNT2_M2	CCACATGGGCTTATATGGCG	TGG	chr1 201346994 201347013
TNNT2_M3	TAGCTTATCTGAGCAGCTGG	AGG	chr1 201347018 201347037
TNNT2_M4	AGGGCTTTAAGCAGGCATGT	GGG	chr1 201346829 201346848
ITGA7_CM1	TGGCTCTGGGAGACGGAACC	AGG	chr12 56099833 56099852
ITGA7_CM2	CCCCCTGCTGGAGCAAAAGC	AGG	chr12 56099774 56099793
ITGA7_CM3	CCACCTGCAACTCAAAGCT	AGG	chr12 56099697 56099716
RDH5_CTCF1	CTGCCACCTGTAGGTCACTT	GGG	chr12 56114938 56114957
RDH5_CTCF2	TTCTGCTGGGTGCCTTACTC	TGG	chr12 56114982 56115001
RDH5_CTCF3	GCTTGAGGGCCACAGTAAAC	TGG	chr12 56114891 56114910

Table S7. Related to STAR Methods. guide RNAs.

Name and sequence of gRNA DNA template, PAM sequence and genomic coordinates.